

Experimental Lab 2: Magnetic Susceptibility

Junior Sophister

Alexandra Mulholland 17336557

February 12, 2020

Contents

1	Abstract	2
2	Scientific Background	2
2.1	The Faraday Balance	2
2.2	The Origin of Magnetic Dipoles	4
2.3	Interaction of Magnetic Dipoles in External Fields	4
2.4	Magnetic Susceptibility	5
2.5	Magnetisation	5
2.6	Diamagnetism	6
2.7	Paramagnetism	6
2.8	Ferromagnetism	7
2.9	Hysteresis	8
3	Method	9
4	Results	11
4.1	Error Propagation	11
4.2	Mohr's Salt	11
4.3	Paramagnetic salt $Gd_3Ga_5O_{12}$	12
4.4	Ferromagnet Hematite $\alpha\text{-Fe}_2\text{O}_3$	14
5	Discussion	15
6	Conclusion	17
	References	18

1 Abstract

Using a Faraday Balance and Hall probe, the magnetic properties of several materials were investigated under the influence of an inhomogeneous magnetic field. Firstly, calibration of the field and field gradient was imperative for later readings upon establishment of the calibration constant. A plot of force due to the magnetic field induced in the solenoids of the Faraday balance versus magnetic field squared for the paramagnetic material $Gd_3Ga_5O_{12}$ did not display the expected trend. The sources of error for which are explored later. However, the magnetisation of said material followed the expected trend: linearly increasing with applied magnetic field. Investigation of the magnetisation of a weakly ferromagnetic material Hematite αFe_2O_3 produced a very narrow hysteresis loop, displaying the anti-ferromagnetic properties of the material.

2 Scientific Background

2.1 The Faraday Balance

In order to explicate the magnetic properties of the materials investigated, it is necessary to explain how the inhomogeneous magnetic field was generated. (1) Faraday's law states that upon application of a magnetic field on a circuit, there will be an induced EMF, which results in current flow. Lenz's law then states that the electric field induced will be in such a direction as to oppose the change in the magnetic field producing it. (2) When formed into a solenoid (as it is for the purposes of this investigation), a current-carrying conductor will cause a magnetic field to be generated as shown in figure 1.

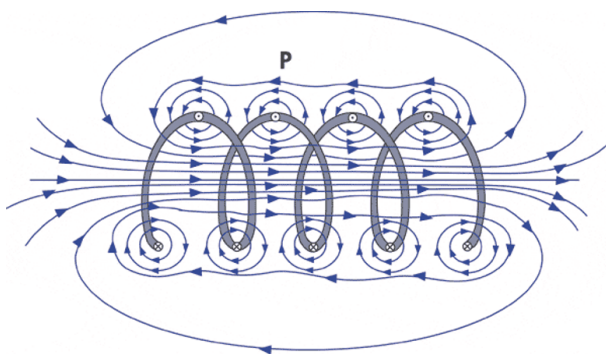


Figure 1: Image of the induced magnetic Field due to a conducting coil

The main component of the apparatus used in this investigation is the Faraday Balance.(13) This consists of two large solenoids with pole pieces known as Faraday pole caps. The inhomogeneity of the field between these two pole pieces is dictated by their shape, whereby along the symmetry axis of the magnet (in the z-direction), the product of the magnetic field (in the x direction) with the derivative of the field in the z direction is constant over a significant range in z. This is shown in equation 1.

$$M = B_x \frac{dB_x}{dz} = constant \quad (1)$$

A balance from which the sample is suspended allows the force to be measured. As will be explained, the magnetic field gradient must be calibrated using a Hall Probe. The sample is to be placed at the position where the Hall probe was, and hence the field gradient is known here. Thus, the magnetic moment of the sample can be easily calculated via the observed force. This will be explained in further detail later. Figure 2 is an image of the setup utilised in the investigation.

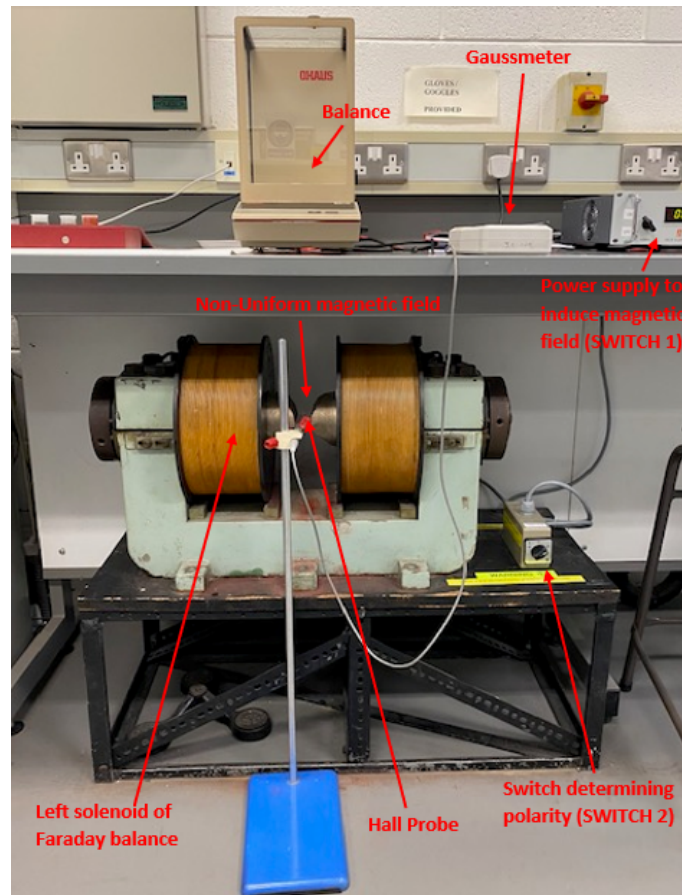


Figure 2: Image of the apparatus used. Labelled are one of the solenoids of the Faraday Balance, the Hall probe (at which position each sample will be placed) which measures the magnetic field, the balance which from which the resulting force will be determined.

2.2 The Origin of Magnetic Dipoles

(1) Determining the origin of the magnetic dipoles which arise in certain materials requires the treatment of the atom classically. This means the electron is viewed as travelling at a radius r from the nucleus at tangential velocity v in circular motion. The motion of the electron constitutes an electric current, i . This current loop possesses a magnetic dipole moment $\mu = i\mathbf{a}$, pointing in the same direction as \mathbf{a} , the vector area of the loop. The current can be represented as in equation 2.

$$i = \frac{-e}{T} = \frac{-ev}{2\pi r} \quad (2)$$

Where T is the period of the electron's orbit and e is the electron charge. The negative sign indicates the direction of the induced current will be opposite to that of the moving electron. Therefore, the dipole moment can be expressed as:

$$\mu = \frac{-ev}{2\pi r} \mathbf{a} = \frac{-e\hbar}{2m} \mathbf{l} \quad (3)$$

Where \mathbf{l} is the angular momentum vector of the orbiting electron, mvr and $\frac{-e\hbar}{2m}$ is known as the Bohr Magneton, μ_B . Equation 3 indicates there is a contribution to an atom's magnetic moment due to the orbit of its electrons. Furthermore, much like the Earth rotates around the sun, the electrons have an intrinsic spin coupled with their orbit. This inherent angular momentum results in a magnetic moment also, contributing double what the orbital momentum does. Summing the total orbital and spin angular momenta over all the electrons leads us to a resulting magnetic moment of the atom:

$$\mu = -\mu_B(\mathbf{L} + 2\mathbf{S}) \quad (4)$$

Should the atom's shells be filled entirely, no electronic contribution to either momenta will result. Thus it is imperative the shells be incomplete for permanent dipole moments to exist and hence the atom act as a miniature magnet, as otherwise net magnetic dipoles may cancel.

2.3 Interaction of Magnetic Dipoles in External Fields

(15) When placed in an external magnetic field, magnetic dipoles will experience a torque which will act to align the dipole parallel to said field. The torque is expressed as $\tau = \mu \times B_{external}$. The potential energy of the dipole, when aligned with the field, will be of the most negative value possible. When the magnetic dipole moment is at an angle to the field, the potential energy will be less negative. The system will naturally wish to reach a lower energy state- one which is more stable. It can be shown that the potential energy of the dipole is negative work done by the field, as shown in equation 5

$$U = -\mu \cdot \mathbf{B} \quad (5)$$

The most favourable energy state occurs when the moment and external field are aligned, as $\cos(0)=1$. Positive work therefore must be done on the dipole to align it in another orientation. A non uniform magnetic field, the force exerted on a dipole is $\mathbf{F} = \nabla(\mu \cdot \mathbf{B}_{external})$. When placed in an inhomogeneous magnetic field acting in the x direction, the force which will act on a dipole is in the negative z direction: $F_z = \mu_z(\frac{\partial B}{\partial z})$. This is the expression utilised for the context of this investigation.

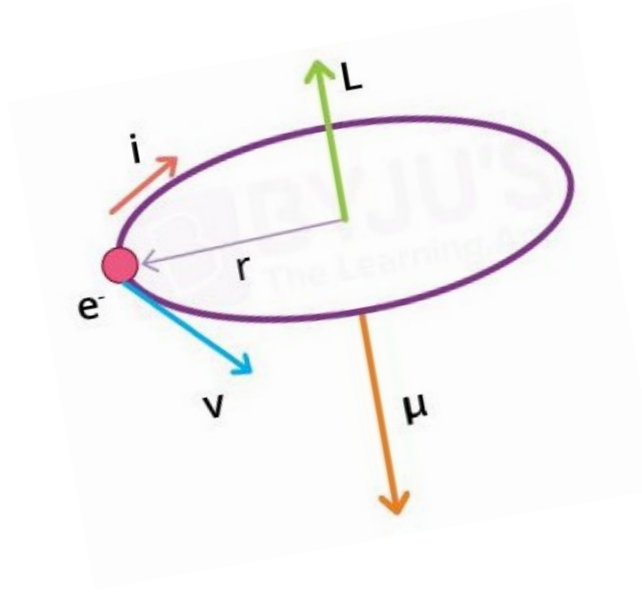


Figure 3: (4) Diagram illustrating the resulting orbital magnetic dipole, μ and orbital angular momentum, L

2.4 Magnetic Susceptibility

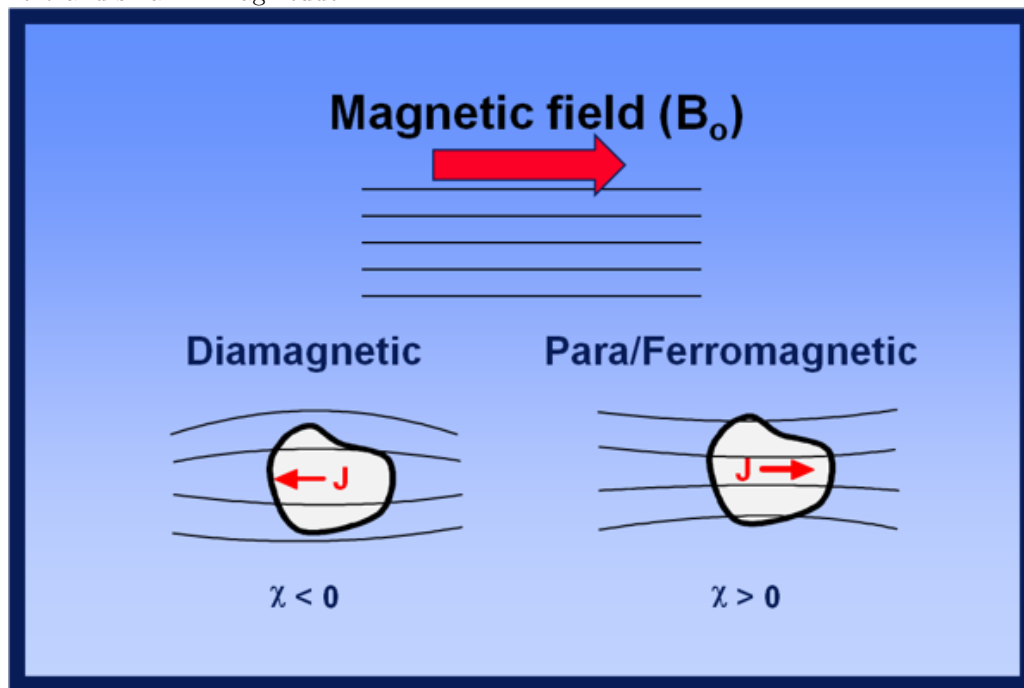
(1) Simply put, the magnetic susceptibility χ quantifies the strength of magnetic effects of a material. The materials investigated are in some way magnetic. Thus, upon application of an external field, the atoms within the material will contribute their internal magnetic fields. (7) It has become common practice to define a quantity known as the magnetic field strength, \mathbf{H} , also known as the macroscopic magnetic field within the material (measured in A/m). $H = \frac{B}{\mu_0} - M$ where M is the magnetisation (elaborated upon later) and B is the magnetic flux density in Tesla. The product of μ_0 and H is the externally applied magnetic field, B_0 . It is useful to expand upon this to elucidate the meaning of magnetic susceptibility. The magnetic flux density can be related to H like so: $B = \mu_m H$ Where $\mu_m = K_m \cdot \mu_0$ i.e the product of the relative permeability of the material and the magnetic permeability of space (respectively). The magnetic susceptibility can be defined via the relative permeability as: $X = K_m - 1$. A material which has a relative permeability value of 1 will not respond to any external magnetic field influence, i.e. its susceptibility is zero.

2.5 Magnetisation

The magnetisation is most commonly defined as the volumetric density of the net magnetic dipole moments. i.e. $\mathbf{M} = \frac{\mu}{V}$. A material whose magnetic dipole moments are all orientated in the same direction will have a high resulting magnetization due to a large net dipole moment. This quantity will be elaborated upon when discussing the various types of materials used.

2.6 Diamagnetism

(2) This type of material is one which has no net magnetic moment. This is because they possess filled electron “shells”. However, when an external magnetic field is applied, the induced magnetisation, M , in the material will be such to oppose the external one. Figure 2.6 exemplifies this behaviour. The susceptibility of such a material, due to its lack of valence electrons, is less than zero and small in magnitude.



(3) Diagram of the induced magnetic field in diamagnetic and paramagnetic or ferromagnetic materials

2.7 Paramagnetism

While all materials have an intrinsic diamagnetic property, some have certain characteristics which will outweigh this behaviour. Paramagnetic materials are ones which exhibit a weak, but positive susceptibility to magnetic fields. This is due to the presence of a small number of unpaired electrons (permanent magnetic dipoles) subject to torque.

(11) These will tend to orient parallel to the applied magnetic field, dominating thermal disorder. Therefore, paramagnetic materials are of small but positive χ . (1) However, upon removal of the magnetic field, no magnetic property is retained, and the configuration of the material is one of randomly orientated spins with no net magnetic moment. The Curie law states the susceptibility of said materials is inversely proportional to temperature.

This intuitively makes sense as at higher temperatures, thermal energies will encourage disorder, and so hinder alignment with the magnetic field applied. This is outlined by equation 6.

$$\mathbf{M} = C \cdot \frac{\mathbf{H}}{T} \quad (6)$$

Where T is the absolute temperature, C is Curie's constant and \mathbf{H} is the magnetic field.

2.8 Ferromagnetism

(7) As previously stated, all materials are inherently diamagnetic. However, if the material exhibits long-range order of magnetic moments (as ferromagnetic ones do) this effect is dominant over the diamagnetic behaviour. In the absence of an external magnetic field, a ferromagnetic material consists of many regions whereby a large number of atomic magnetic spins are aligned in parallel. These regions are known as domains, which are oriented in different directions and classified by strong exchange coupling of the individual microstates.(2) Due to the random orientation of said domains, the material will exhibit a zero net magnetic moment. When a magnetic field is applied, these domains will align forming one single domain, thus the material will now exhibit a non-zero net magnetism. The domain boundaries mark the separation of contrasting spins. The resulting torque from both the external magnetic field and the dipole moments of neighbours means the spins will be re-oriented to align with the magnetic field. Those domains whose spins are primarily aligned with the magnetic field will consequently enlarge. Due to this response to an external magnetic field, ferromagnetic materials evidently have a large, positive susceptibility, χ . Figure 4 shows a crude illustration of the dipole moments of the constituents of each material type, while figure 5 shows the magnetic susceptibility trends for each of the three types of material.

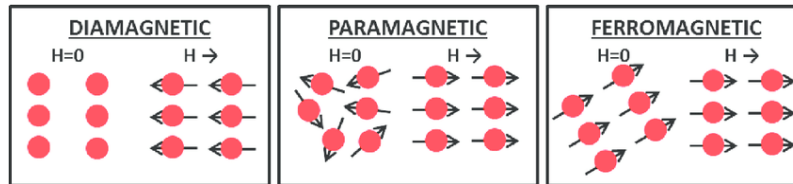


Figure 4: (8) Image of the spins of dia-, para- and ferromagnetic materials (Here only one domain of a ferromagnetic material is illustrated)

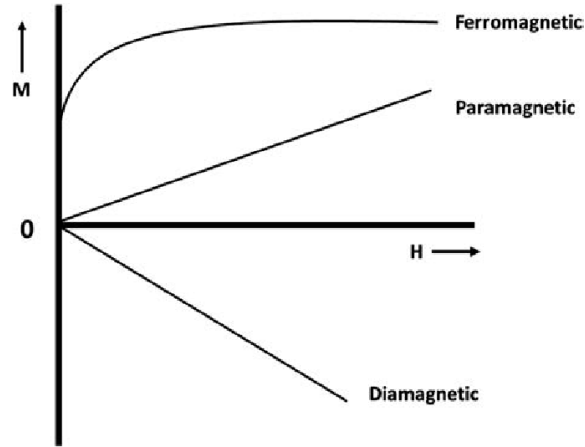


Figure 5: (9) Plots of the Magnetic Susceptibility versus applied magnetic field for ferromagnetic, paramagnetic and diamagnetic materials.

2.9 Hysteresis

(14) Upon removing the externally applied magnetic field which magnetised a ferromagnetic material, the magnetisation will not return to zero. In the context of this investigation, a hysteresis loop was plotted through the application of a varying potential difference (and hence alternating magnetic field). The magnetisation of the material, when plotted against the applied magnetic field, will trace out said loop and is impossible to retrace upon magnetic field reversal. The Hall effect sensor allows detection of the magnetic field, and the Faraday Balance allows for determination of the force. For a ferromagnetic material, the force acting on the dipoles due to the magnetic field is given by equation 7.

$$F_z = m\sigma CB_x \quad (7)$$

Where m is the mass of the sample. Figure 6 shows a hysteresis loop for an arbitrary ferromagnetic material.

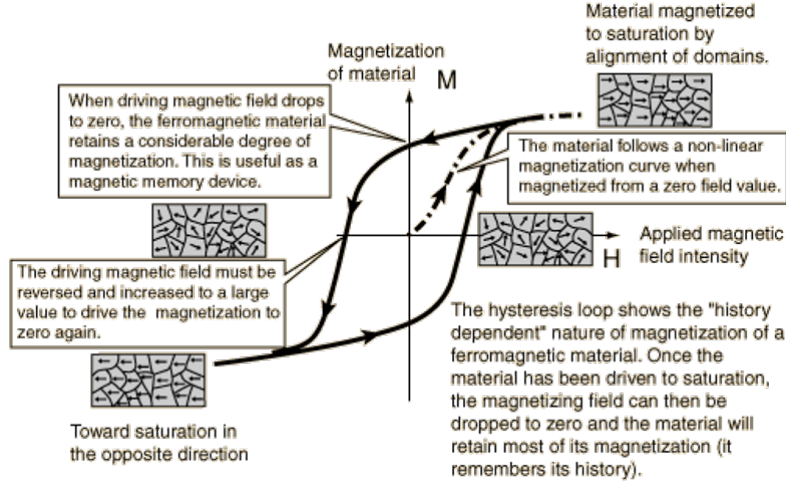


Figure 6: (14) Hysteresis Plot for a ferromagnetic material

3 Method

Before commencing experimentation, the appendix on how to handle the materials used in this investigation should be read and the guidelines followed. Furthermore, the magnetic field and magnetic field gradient must be calibrated. Care must be taken upon commencing as there are risks of damaging the coil or power supply and hence rendering the experiment inexecutable. For instance, it is essential that the current is at 0.0A before turning the power supply on or off. The coil used to generate the inhomogeneous magnetic field is evidently very large and improper use of the power supply could result in an extremely large back EMF.

Switch 1 shown in figure 2 supplies power to the coil. Switch 2 controls the polarity of the magnetic field induced: forward or reverse (Done so by altering the direction of the current which induces it). Before commencing, switch 2 must be set to the 'OFF' position. To reiterate, the voltage and current readings must be at zero- i.e. the dials must be fully anticlockwise. Once these conditions are met, the power supply (switch 1) may be turned on. Using the 'DISPLAY SETTING' button, the maximum current limit on the power supply is set to 10.00A. This is to prevent damage to the apparatus through application of a voltage which is too high.

Next, the Hall Probe, which detects the magnetic field being applied to the sample, is placed centrally between the poles of the solenoid. This is the closest position to which the sample will be positioned. The Gauss Metre is connected to the probe so a reading of the magnetic field may be taken. Now the apparatus has been set up to calibrate the field, switch 2 is set to the initial polarity desired ('FORWARD'). Current is then permitted to flow from the power supply to the coil to produce a magnetic field. The voltage across the coil is then slowly increased from 0.0V with the voltage dial in intervals of 5.0V. The corresponding current and magnetic field are recorded until a value of 85.0V is reached. At this point, the voltage is then reduced to 0.0V in the same intervals, with the current and magnetic field recorded again.

When 0.0V is obtained, the polarity of the magnetic field is switched to 'REVERSE' and the procedure is repeated, recording the corresponding current and the (now negative) magnetic field.

Once completed, and both the voltage and current read zero, the coil ‘SWITCH 2’ is set to the ‘OFF’ position. The Power supply is then switched off to stop current flow to the coil. The results for forward and reverse polarity of the magnetic field are then plotted on a graph of magnetic field (mT) versus current (A). This concludes the calibration of the magnetic field. Next, calibration of the magnetic field gradient must be executed. This is done using a sample of Mohr’s salt. In order to measure the force due to this magnetic field, a sensitive weighing scale is utilised. Attached to the plate of said scale is a wire with a holder at the end which will hold the sample. Initially, its mass is measured (with no sample inside), and the result is recorded. Using tweezers, some of the salt was added to the sample holder and the new mass is recorded. It is essential that a large enough mass is added to observe the effect of the magnetic field on the material, but not too large so that the material is attracted to one of the poles substantially (whereby the sample may stick to it). It should be noted that there is likely to be a remnant magnetic field from the calibration, which could result in an increased apparent weight than its actual value.

Nevertheless, the calibration constant for this apparatus can be determined using the equation $F_z = Cm\chi B_x^2$ where the mass and susceptibility ($\sigma = 0.33JT^{-2}kg^{-1}$) of Mohr’s salt are known. By measuring the voltage, forward current and corresponding magnetic field (increasing voltage from 0.0 to 85.0V in 5.0V intervals), one can plot a graph of F_z versus B_x^2 and determine the gradient, which is $Cm\chi$. The calibration constant value can thus be used in later parts of the experiment to deduce the susceptibility and magnetisation of a paramagnetic and ferromagnetic material respectively. It is imperative that all the samples be placed in the same position between the solenoid, as on which the calibration constant depends. Now, a paramagnetic material $Gd_3Ga_5O_{12}$ can be investigated, for which the magnetic susceptibility is unknown. The mass of the holder is measured again as there may be variations due to the downward force acting on the apparatus. Tweezers are used and again, the voltage is increased from 0.0 to $85.0 \pm 0.05V$, in intervals of 5.0V, with the corresponding magnetic field is measured and recorded. (1) The value of the susceptibility can then be deduced from the gradient and compared to the expected value given by 8.

$$\chi = \frac{Ng^2\mu_B^2J(J+1)}{3kT} \quad (8)$$

Where N is the number of magnetic ions per kg of the sample, g is the Lande g-factor, μ_B is the Bohr magneton, J is the orbital quantum number, k is Boltzmann’s constant and T is the temperature.

Finally, a graph of force versus magnetic field for a weakly ferromagnetic material, hematite, was plotted. As for the calibration of the field, the voltage was increased from 0.0 to 85.0V in 5.0V intervals, then decreased to 0.0V for the forward polarity, and then repeated for reverse polarity. Corresponding values of current, magnetic field and change in mass (and hence resulting force) were measured and recorded. From these values of force and magnetic field, along with the mass and calibration constant being known, values for the magnetic moment per unit mass can be deduced at each current interval. A hysteresis plot of sigma versus magnetic field is then graphed.

4 Results

4.1 Error Propagation

Error in χ for paramagnetic salt:

$$\chi = \frac{\text{gradientvalue}}{mC}$$

$$\Delta C = \pm 0.016\%,$$

$$\Delta m = \pm 0.06\%,$$

$$\Delta_{grad} = \pm 0.108 = 4.45\%$$

$$\delta\chi = \chi \left(\sqrt{\left(\frac{0.00007}{0.1134}\right)^2 + \left(\frac{0.00216}{12.9}\right)^2 + \left(\frac{0.1079}{2.42}\right)^2} \right) = \pm 0.06$$

4.2 Mohr's Salt

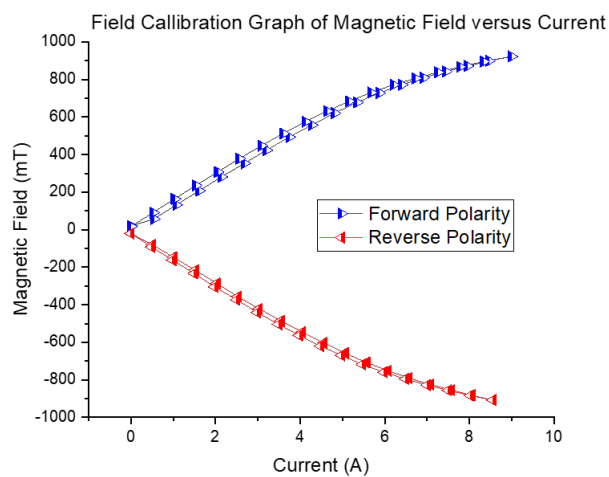


Figure 7: *

Figure 1.0: Field calibration Graph of Magnetic Field induced versus Current applied to the Faraday Balance

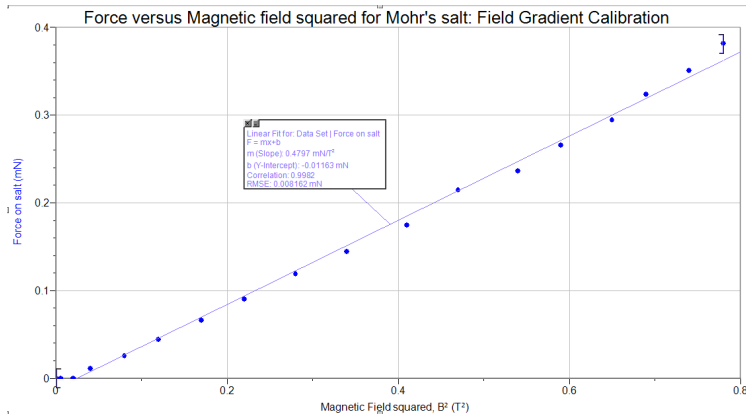


Figure 8: *

Figure 1.1: Field Gradient Calibration plot of Force acting on Mohr's salt versus the magnetic field induced

4.3 Paramagnetic salt $Gd_3Ga_5O_{12}$

labelformat=empty

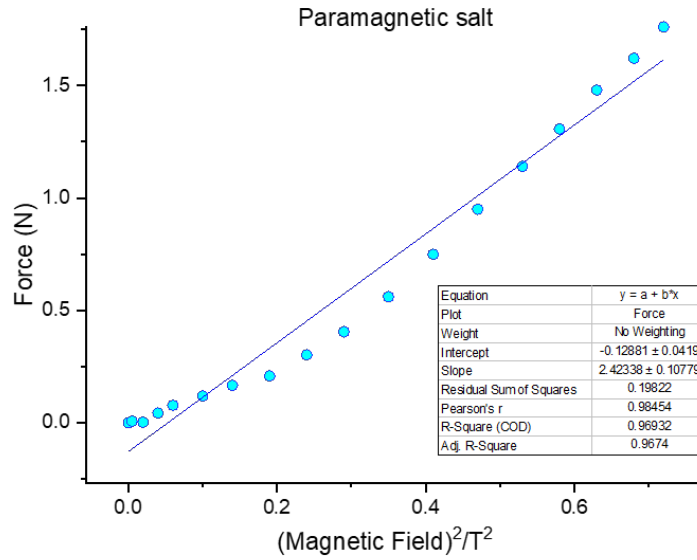


Figure 9: *

Figure 2.1: Plot of Force acting on the paramagnetic salt sample versus magnetic field squared

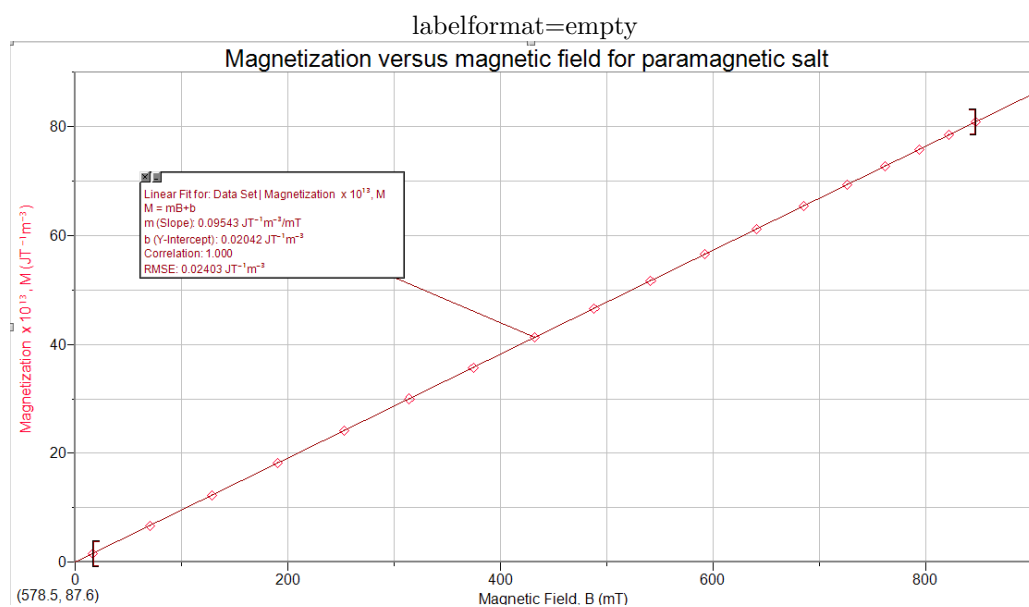


Figure 10: *

Figure 2.2: Plot of the Magnetisation versus Magnetic field for the paramagnetic salt, Gallium Gadolinium Garnet

4.4 Ferromagnet Hematite $-\alpha Fe_2O_3$

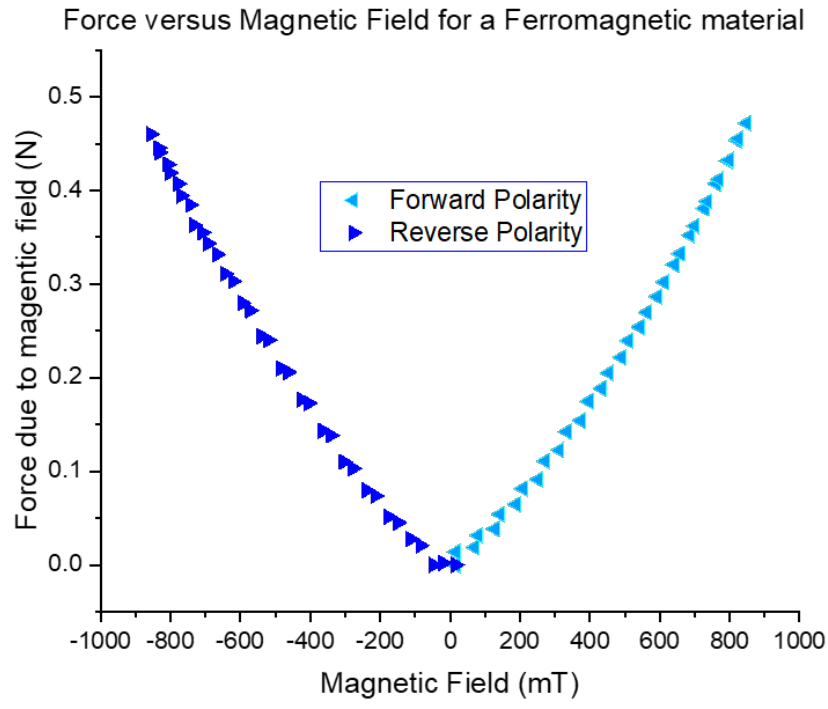


Figure 3.1: Plot of Force versus Magnetic Field strength for a ferromagnetic material Hematite $-\alpha Fe_2O_3$

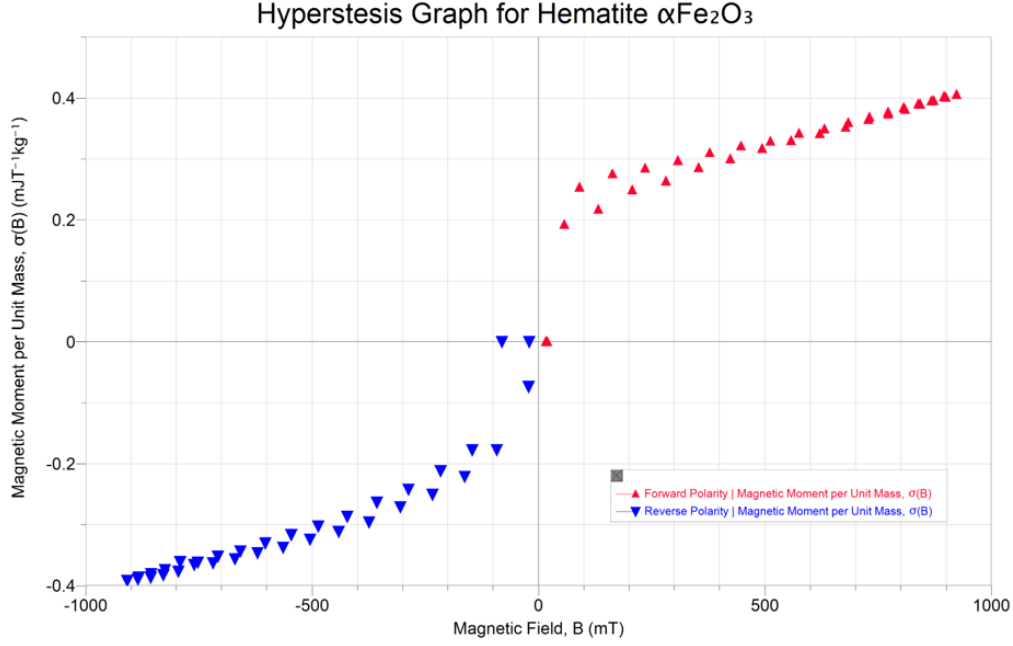


Figure 3.2: Hyperstesis Trend for Hematite $\alpha\text{Fe}_2\text{O}_3$

5 Discussion

Figure 1.0 displays the Calibration graph for the magnetic field applied versus current. First, the voltage was increased from 0.0 to 85.0V in steps of 5.0V. Then, this voltage was decreased to 0.0V again in the same intervals and the magnetic field reversed. The process was then repeated, recording magnetic field and current at each step. This was necessary as for later parts of the experiment, reference to the calibrated magnetic field was needed for certain voltage values. For the purpose of simplicity, the current intervals were kept consistent so as to use the same magnetic field values, B_x , as were measured upon calibration. One will note the graph is not quite a linear fit. This could be a result of the system not having warmed up sufficiently to reach a consistent resistance value for a prolonged period of time. Figure 1.1 shows the magnetic field gradient plot calibrated using Mohr's salt.(10) Such a material contains two different cations: Fe_2^+ and NH_4^+ and is often used for calibration in this context. Knowing the magnetic susceptibility to be $\chi = 0.330 \text{ JT}^{-2} \text{ kg}^{-1}$, one can determine the calibration constant, C, used in subsequent parts of the experiment. This is done using the equation of the force from the magnetic field acting on the salt: $F_z = C m \chi B_x^2$. The mass of the salt was measured to be $0.1134 \text{ g} \pm 0.06\%$. Rearranging the equation, the calibration constant was found to be $\approx 12.9 \text{ m}^{-1}$.

Figure 2.1 shows the force in Newtons ($\times 10^{-3}$) versus the magnetic field squared in accordance with the force acting on a paramagnetic material of mass $0.1375 \pm 0.00007 \text{ g}$. From the gradient, which is $C \chi m = 2.42 \text{ gms}^{-2} \text{ T}^{-2}$, the susceptibility was experimentally found to be $\chi = 1.36 \pm 0.06 \text{ m}^2 \text{ s}^{-2} \text{ T}^{-2}$. From 8,(1) using $N = 1.78 \times 10^{24} \text{ kg}^{-1}$, $\mu_B = 9.27410^{-24} \text{ JT}^{-1}$, $J = \frac{7}{2}$, g-factor=2 and $T = 293.15 \text{ K}$, one can see this experimental value is significantly higher than expected: $\chi = 0.79 \text{ JT}^{-1} \text{ kg}^{-1}$), being outside the range of error permitted.

This is most likely due to error in calibration and misuse of equipment, as calibration and paramagnetic salt reading were taken on separate days. One can see from the trend the plot is not linear, rather more exponential. This could be due to the system not being allowed to warm for a sufficient time for the resistance to reach the value of 10ω as it had on the first day of experimentation. Furthermore, as is noted in the lab book, the instrumentation was left at 85.0V for a significant period of time and so a much larger magnetic field was permitted to build than necessary.

Out of interest, the magnetisation values for the $Gd_3Ga_5O_{12}$ were calculated and plotted against applied magnetic field to see if the results followed those outlined in figure 5. Figure 2.2 shows a clear linear trend, with a small positive gradient. This is as expected for a paramagnetic material, whose dipoles will overcome thermal disorder to align with the magnetic field applied.

Figure 3.1 was plotted to elucidate the behaviour of the force, F_z acting on the ferromagnetic material, Hematite αFe_2O_3 . The results are as expected, with the magnitude of the force downwards increasing on the material with magnetic field for either polarity.

Figure 3.2 shows the hysteresis loop for the ferromagnetic sample of mass $0.1063g \pm 0.06\%$. One will observe this is a very narrow loop in comparison to example plots. This indicates that, upon removing the driving field, the material does not retain much of the saturation magnetisation. The area enclosed within the loop is indicative of the amount of energy dissipated upon reversal of the magnetic field. The narrowness of the loop implied a small amount of energy is dissipated when repeatedly reversing the field. An interesting note is, while this material is evidently unsuitable to serve as a permanent magnet, it would be very useful for motor cores. This is because the application of AC currents to such a material results in a minimal energy loss and hence increased efficiency. The value of the saturation magnetization on average was calculated to be $0.4319mJT^{-1}g^{-1} \pm 4.73\%$. Estimating from the figure, the remnant magnetisation upon reducing the magnetic field to zero Tesla is approximately $0.19mJT^{-1}g^{-1}$. The coercive force required to reduce the magnetisation of Hematite to zero again is approximately $100 \pm 10mT$ in magnitude. The narrowness of the loop can be explained by the fact that this sample of hematite is not a true ferromagnet, but rather a 'canted' antiferromagnet. In such a material, neighbouring spins are aligned antiparallel to one-another. The resulting net magnetic moment is subsequently much less, and so the remnant magnetisation will be much less also.

6 Conclusion

Overall, the experiment was successful in outlining the intricacies of various magnetic materials. The calibration graph, while showing the results expected, may have been unrepresentative of the magnetic field which was truly acting on each sample. The resistance of the system was found to have increased from 10.0ω to $10.8 \pm 0.09\%$. This may have lead to the undesirable trend observed for the paramagnetic salt. Review of the methodology is required to obtain more reliable values. From the magnetic field gradient calibration of Mohr's salt, the calibration constant calculated was significantly lower relative to similar experimental values, being $\approx 12.9 \pm 0.0022m^{-1}$. Subsequently, the susceptibility value for the paramagnetic sample was substantially higher than expected, at $1.36 \pm 0.06m^2s^{-2}T^{-2}$. However, the magnetisation plot for this sample followed the expected trend, showing a shallow, positive gradient. From the hysteresis plot for hematite, it is clear the material is not a true ferromagnet. The narrowness of the loop indicates little energy dissipation upon varying the magnetic field. The material is actually of much smaller magnetic susceptibility due to the antiparallel alignment of the microstates. Small error may have been contributing throughout the experiment where remnant magnetic field was affecting each sample's initial mass value. Hence, the results obtained are not truly representative. However, overall the results behaved as expected and highlight the behaviour of the materials well.

References

- [1] Hook, J.R., Hall, H.E. *Solid State Physics*. Wiley, Chicester, 1974
- [2] NDT Resource Centre *Hyperstesis Loop*. Iowa State University. (2001-2014)
- [3] Elster LLC. *Magnetic Susceptibility*. Questions and Answers in MRI, 2019.
- [4] BYJU's Learning app. *Diamagnetism, para-magnetism and ferromagnetism*. <https://byjus.com/physics> (2014)
- [5] Ramsden, E. *Hall-effect Sensors: Theory and applications (2nd Ed.)*. Amsterdam. Elsevier/Newnes p. 195 (2006)
- [6] Richtberg, S. *Electron Motion in Electric and Magnetic Fields*. LMU Munich- Chair of Physics Education.
- [7] Carl, R. *Magnetic Field strength H*. Department of Physics and Astronomy. Georgia State University
- [8] Leonardo Ricotti *Magnetic Field-Based Technologies for Lab-on-a-Chip Applications*. (June 2016)
- [9] Chaudhary, V. *Magnetic Nanoparticles: Synthesis, Functionalization and Applications*. (November 2018)
- [10] N. Greenwood, A. Earnshaw *Chemistry Of Elements (2nd ed.)*. Butterworth-Heinemann
- [11] Arvind Singh Heer *Magnetism*. Msc-I. Mithibai College. LinkedIn
- [12] H.B. Gray, R.L. Dekock *Chemical Structure and Bonding*. (2020)
- [13] Dr. J. C. P. Klaasse *The Faraday Balance*. Van Der Waals-Zeeman Institute, November 1999
- [14] Chemistry Libre Texts *Magnetic Hysteresis*. (2018)
- [15] Enriched Physics Lecture notes *Magnetic Dipoles*. www.phys.ufl.edu (2017)